The Chemical Composition of Globules B and C in the Helix Nebula

Lucille Steffes[1, 2], Jesse Bublitz[2]
[1]*University of Wisconsin, Madison*
[2]*Green Bank Observatory*

Abstract

This project seeks to examine the structure of two small, dense clumps of gas, called globules, inside of the Helix Nebula. A series of twelve molecular transition lines were studied, including isotopologues. The two globules studied, Globules B and C, are found inside of the ionized region of the planetary nebula, a habitat otherwise not suitable for molecular formation or survival without significant shielding. Examining the integrated intensity, column density, and velocity distribution indicates that higher densities are found closest to the central star, with more diffuse gas trailing radially outward, while examining the line ratios of molecules detected at multiple transitions suggest that higher energy transitions are more readily excited towards the white dwarf-facing surface of the globule, with lower transitions being more widespread.

1: Introduction

1.1: Background

The Helix Nebula (NGC 7293) is a planetary nebula- the outer remnants of a dying low mass star. Surrounding the white dwarf star seen in the center of the image of the Helix Nebula is a layer of highly irradiated diffuse ionized gas, as seen in blue, which indicates emission from O III (*Figure 1*). The outer layers, seen in white and yellow, are comprised of higher density gas and dust, with the red outermost layer being nitrogen and Hα.

The focus of this project has been two clumps of gas, called globules, found inside of the ionized region of the planetary nebula. This environment is generally extremely destructive to molecular bonds, preventing molecular formation or survival outside of regions shielded by dense clumps of gas due to direct ultraviolet radiation from the central star of the planetary nebula (CSPN). The UV radiation from the white dwarf star tends to break molecular bonds before they have enough time to accumulate and self-shield in a manner that is effective enough to lead to a small and dense

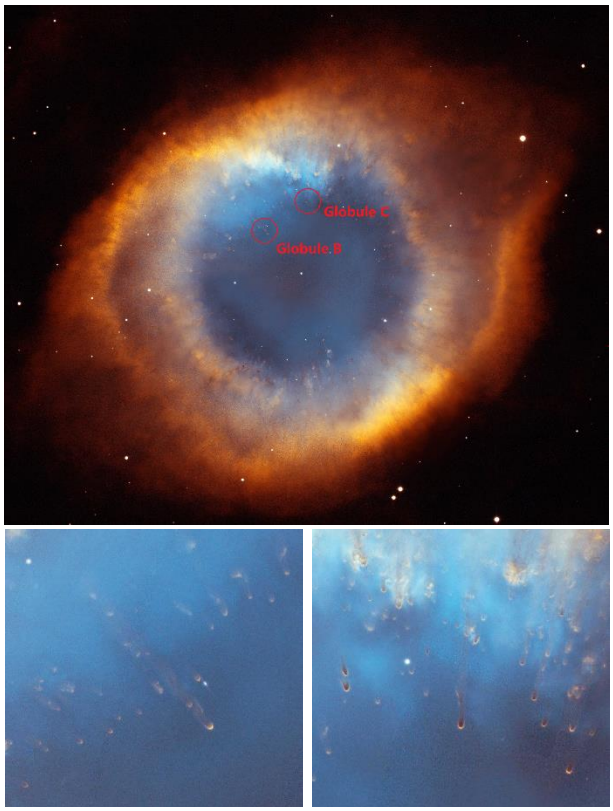

Figure 1: The Helix Nebula and Globules B and C
Hubble image of the Helix Nebula (above) (NASA, NOAO, ESA, the Hubble Helix Nebula Team, M. Meixner (STScI), and T.A. Rector (NRAO).) with two denser globular regions circled in red. Zoomed in panels of Globules B (lower left) and C (lower right) reveal the clumpy structure of the cold non-ionized gas embedded throughout the planetary nebula.

cloud as is found with Globules B and C. Globules B and C are two of the largest globules found in the Helix Nebula, with Globule B the nearest globule to the CSPN, and Globule C found directly North of the CPSN.

1.2: Methods

Data was collected using the Atacama Large Millimeter Array (ALMA) in Cycle 7 in 2019. The reduced data provide three-dimensional data cubes of emission in the plane of the sky, as well as the targeted frequency band. The frequencies were each converted to velocity using the respective rest frequencies. Each file was cropped at the same right ascension and declination values based on the location of the region of high emission from all the molecular species. This accounted for differences in pixel size and reduced the noise seen around the edges of the images. To further reduce the noise, only the channels with statistically significant emission were used in maps and calculations. A mask was also applied to pixels below a 3σ threshold. The CO data for Globule C was ALMA archival data (*Cycle 2, PI: P. Huggins*), which was more recently analyzed and published (*Andriantsaralaza et al., 2020*).

2: Integrated Intensity

2.1: Moment 0 Maps

The Moment 0 maps, (*Figures 2-3*) illustrate the integrated intensity, which sums along the frequency axis, creating a two-dimensional representation of the three-dimensional data cube. The Moment 0 maps were produced by integrating along the frequency axis for each pixel in the region along the plane of the sky:

$$\text{Moment 0} = \int I_v \, dv \qquad (1)$$

The relevant channels are also illustrated in the individual velocity channel maps (*Figure 4*). The selected individual velocity channel maps, the 1-0 transition for HNC for both Globules B and C also illustrate the relative location of each of the features seen in the corresponding Moment 0 maps (*Figures 2-3*). The individual velocity channel maps also show that Globule B spans a larger range of velocity channels than Globule C, spread across 4 channels from -17.63 to -16.20 kms^{-1}. This indicates that the gas is projected out of the plane of the sky yet remaining directed away from the CSPN. Conversely, Globule C spans 3 channels from -28.34 to -27.41 kms^{-1}.

The brightest areas in the Moment 0 maps, where emission intensity is highest, appear in the heads of the globules, closest to the CSPN. Trailing away from the CSPN, the intensity decreases. ^{12}CO and ^{13}CO are widespread across both globules, illustrating the shape and limits of the outer edges of the globules. $C^{18}O$ is constrained to a narrow region of the main head closer to the CSPN. This stratification is likely due to the extreme differences in the isotope ratios for ^{12}C to ^{13}C and ^{16}O to ^{18}O (*Andriantsaralaza et al., 2020*). $C^{18}O$ is the least common of the CO isotopologues detected, only found in the densest regions of the globule. $C^{18}O$ is the least common of the CO isotopologues because ^{18}O is far less common than ^{16}O, at a ratio of $^{16}O/^{18}O=115$ (*Andriantsaralaza et al., 2020*). Additionally, ^{18}O is readily dissociated into ^{16}O, with ^{18}O only being produced in the AGB phase, so the most $C^{18}O$ would be found in the densest regions where shielding is the greatest (*Andriantsaralaza et al., 2020*). Unlike $C^{18}O$, the other molecules have higher intensities further up into the tail of Globule B. HC_3N and C_2H are found in isolated bright spots tracing the tail of Globule B, with the rest of the molecular detections being more widespread.

Figure 2: Moment 0 Images for Globule B

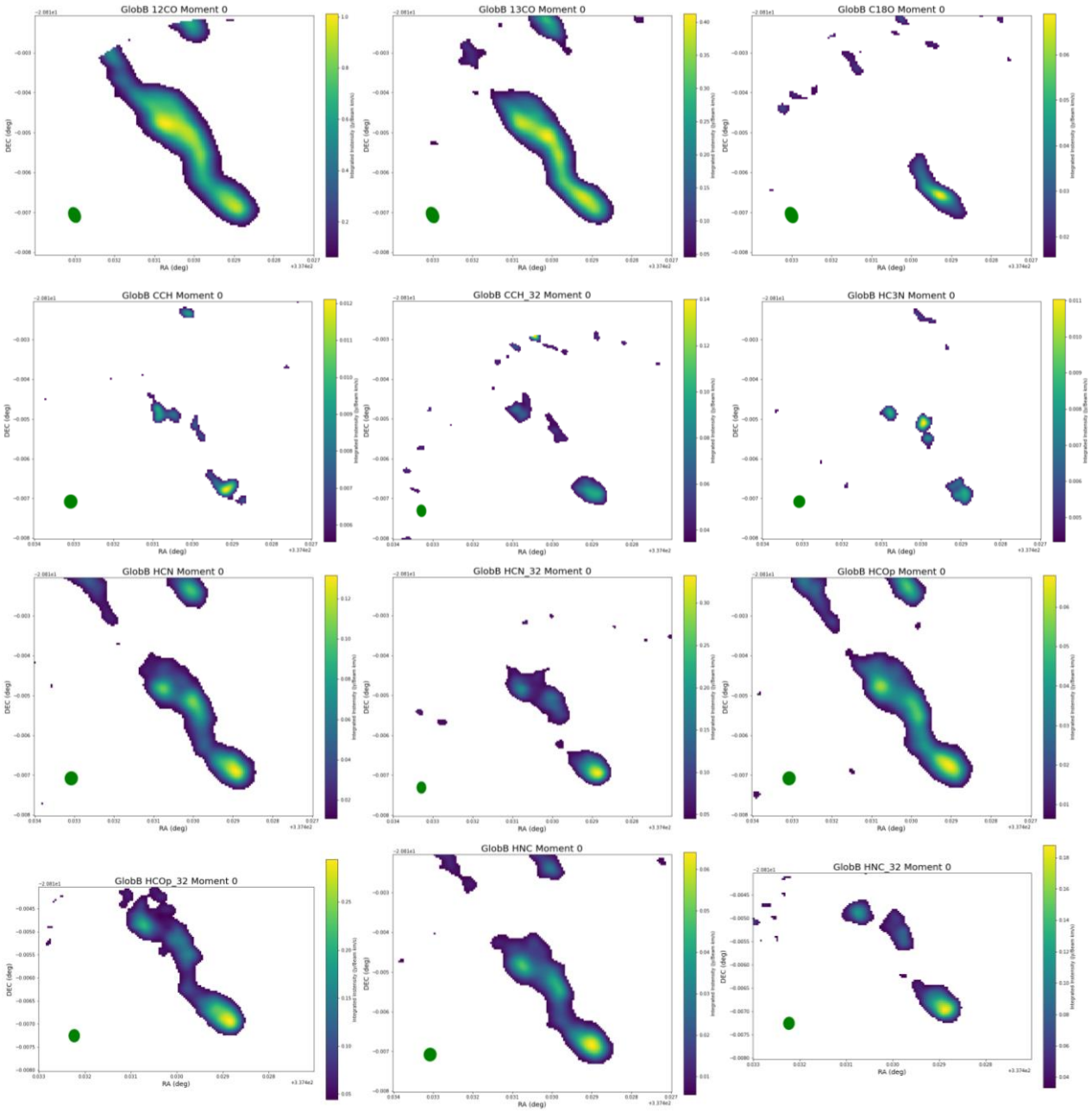

The Moment 0 maps for Globule B show the integrated intensity over relevant channels, with the yellow representing the areas with the highest intensity emission.

Figure 3: Moment 0 Images for Globule C

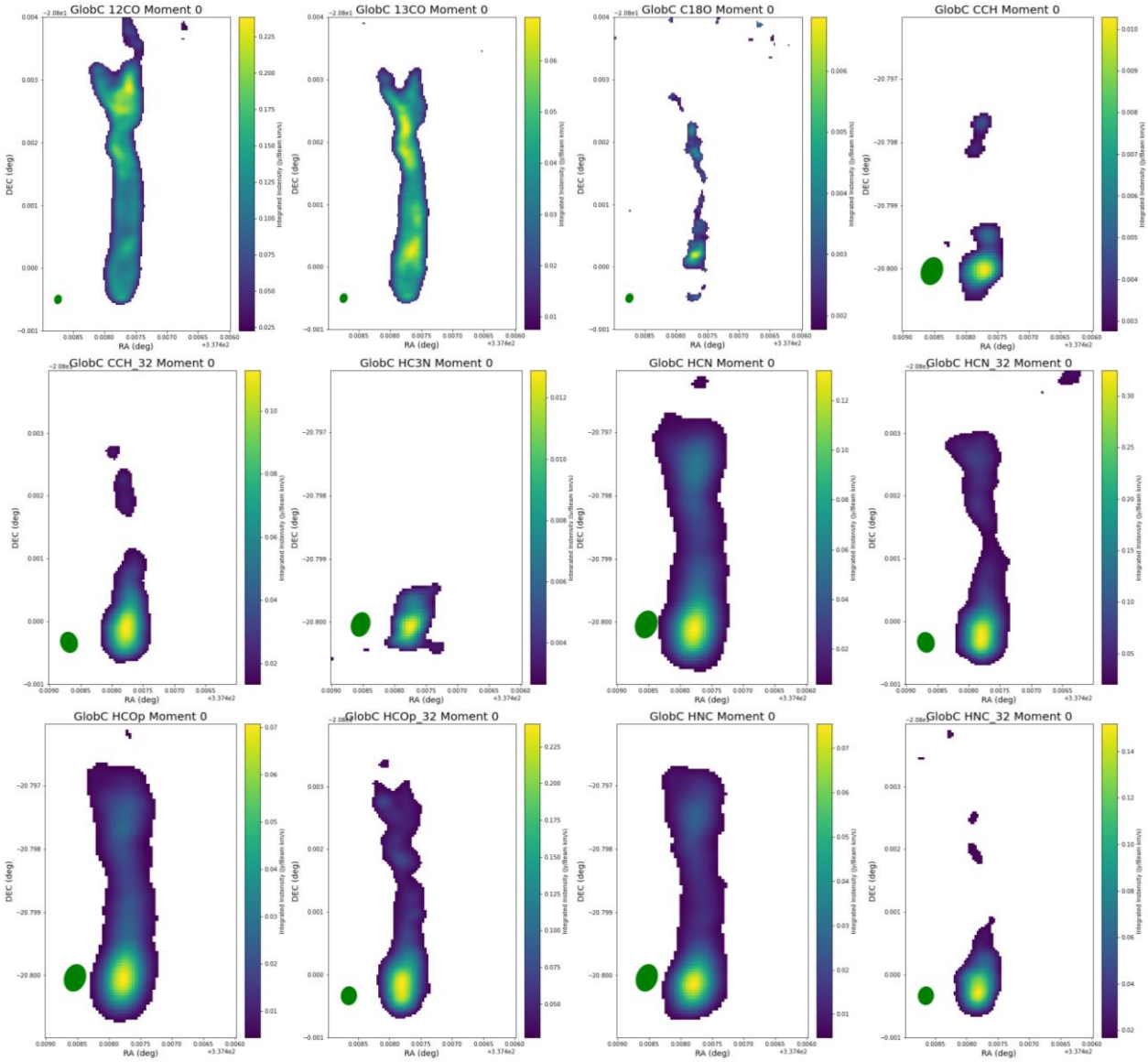

The images above show the Moment 0 maps for Globule C with higher intensity emission being shown in yellow.

Extended maps afforded by a larger field of view for lower frequency lines reveal smaller globules, each with a distinct head, referred to as globulettes. The Helix Nebula contains an estimated 26,000 globulettes, though one does appear to merge with Globule B. This globulette, just north of Globule B, does not extend much further back than the images in *Figure 2* indicate. While the tail of Globule B extends beyond the images, the extent cannot be ascertained here. In extended maps, it is possible to see globulettes around the primary globule being studied, though fewer globulettes are seen surrounding Globule B than Globule C. Each of the globulettes detected appear more concentrated in the heads of the globulettes with no visible within a 3σ detection, having a much smaller size and a lower intensity than Globule B or C.

Figure 4: Individual Velocity Channel Maps

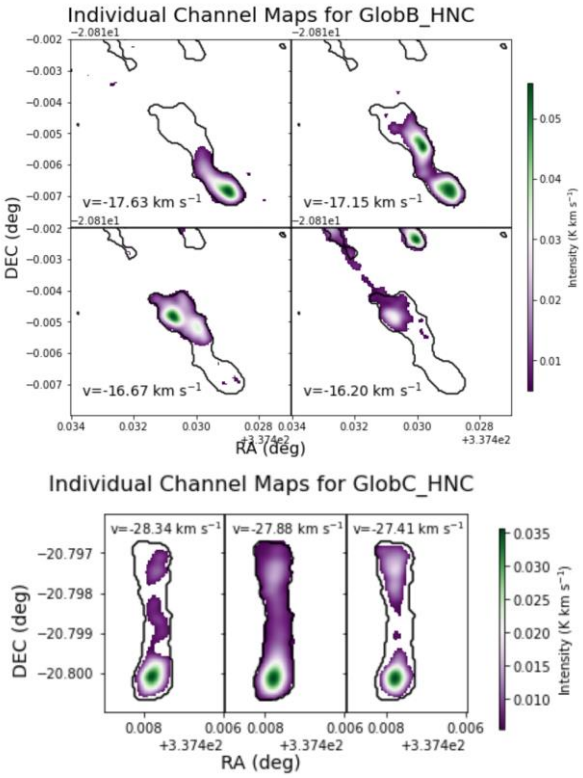

Individual channel maps for Globule B (above) and Globule C (below) for 3σ of emission detected in HNC.

2.2: Comparative Structure

The comparative contour maps (*Figure 4)* illustrate the edges of each of the twelve 3σ molecular detections. Six points in Globule B and two in Globule C have been identified as the brightest pixels in HCN within each region. They were chosen based on the integrated intensity for HCN due to it being optically thin yet extended. Point 3 in Globule C was chosen when examining the column density map for ^{12}CO, which featured an abnormally bright spot west of the fork in the tail, suggesting further investigation. The clustering of the contours highlight three distinct structures in Globule B. The clusters predominantly come from less expansive molecules (HC_3N and C_2H) which contain only a head and several smaller spots in the tail. The comparative structure map for Globule B illustrates that these regions overlap where there were bright spots in the tails of the Moment 0 maps, again indicating three interconnected globulettes, with individual heads and tails that merge into a continuous structure.

Figure 5: Contour Comparison Maps

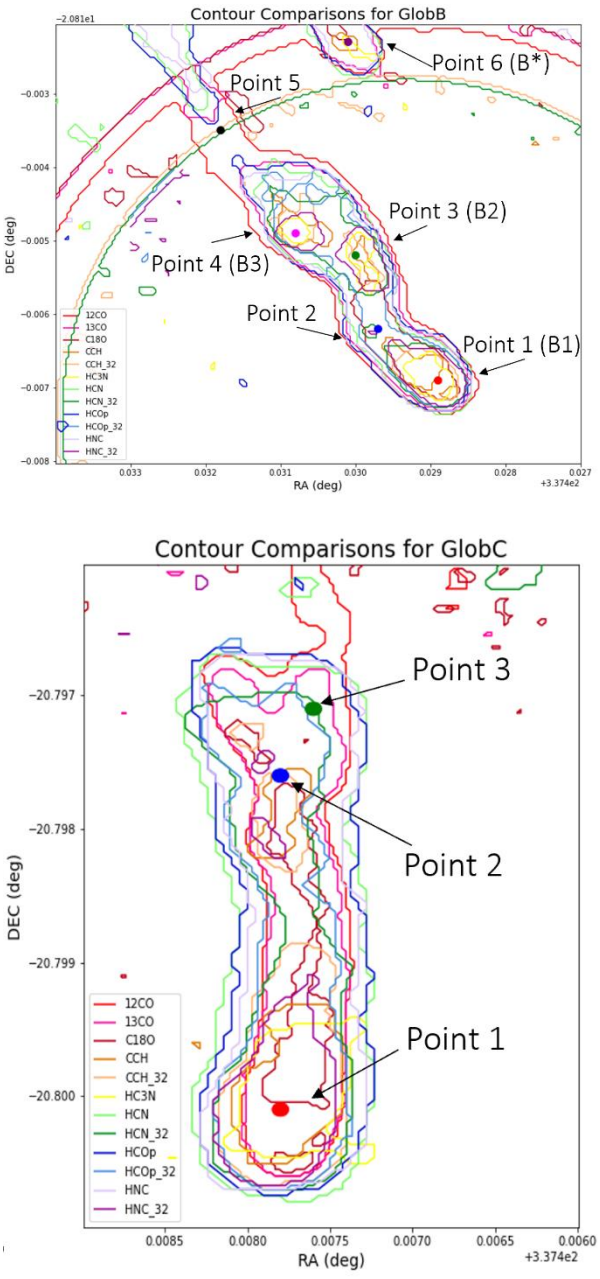

Comparisons of the edges of the 3σ detections of the 12 molecular emissions of Globule B above and Globule C below.

In Globule B, three of these bright spots have been identified (*Figure 5*). The head of the main structure, assumed to be the main substructure of Globule B, is labeled as Globulette B1, with the two following substructures being referred to as B2 and B3. The small emission feature north of the main structure for Globule B, Globulette B*, appears to run parallel to Globule B and is more visible in extended maps using lower frequency transitions.

The contour comparison of Globule C (*Figure 5*) is simpler than that of Globule B, with a single dense head and a lack of consistent substructures in the tail. The contours of Globule C also indicate differences in the distribution of the molecules, with HC_3N and C_2H clustered in the head and $C^{18}O$ spanning the length of the globule, confined to the middle right ascension values. There are also some smaller overlapping substructures in the tail, though none of them appear to be separate globulettes, rather exceedingly small clumps of gas in the same regions, a pattern which does not continue into the more expansive molecules' Moment 0 maps.

3: Velocity Distribution

3.1: Moment 1 Maps

The Moment 1 Maps illustrate the velocity structure of the globulettes within the 3σ detection of the molecule (*Figures 6-7*) using the equation:

$$\text{Moment 1} = \int v^2 I_v \, dv \qquad (2)$$

The Moment 1 maps for Globule C are generally uniform throughout the entire globule, indicative of its nearly vertical in the plane of the sky and within the greater structure of the Helix Nebula.

The Moment 1 maps for Globule B further suggest that multiple globulettes make up the larger structure of the globule. Globule B starts off blue-shifted in the head, and progresses toward a redshift in the tail, demonstrating that Globule B is angled away from the observer on Earth. It is also clear that there is a red shift in the tail, specifically a color distinction between the globulettes B1 and the two further up in its tail, B2 and B3. This change in color is also more apparent in the molecules with higher frequencies that are predominantly confined to the heads of the globulettes, such as the $J = 3 \rightarrow 2$ transition for HCN, HCO^+, HCN, and C_2H. In these images, it is apparent that the globule is both angled slightly away from the observer, and is comprised of several different pieces, observed at several distinct velocities.

The Moment 1 Maps for Globule C indicate the more cohesive structure of a larger single knot of gas as compared to Globule B The Moment 1 maps for every molecular transition contains the same spread of velocity range demonstrating that the distribution of velocities for the molecules in Globule B are the same. the distribution of the molecules about the radial axis of the globule is symmetric and evenly distributed.

3.2: Spectra and Hyperfine Transitions

The spectral lines are made by depicting the total emission from each velocity channel in a line graph (*Figures 8-9*). Most of the molecular transitions feature a single peak at the velocity calculated from the rest frequency of the transition and the central velocity of that globule. From the spectral lines, the average central velocities for Globules B and C are -17.01 km s^{-1} and -27.99 km s^{-1}, respectively. The strength of the signal relates to the Moment 0 maps, effectively

showing the same thing in different ways. Where the Moment 0 maps showed the integrated intensity as color on a sliding scale, the spectral lines show the intensity for each velocity channel as the height on the graph. In the cases where the signal to noise ratio is much lower, the signal is weaker in most of those areas, correlating with the transitions detected over a smaller area after the 3σ masking.

Figure 6: Moment 1 Maps for Globule B

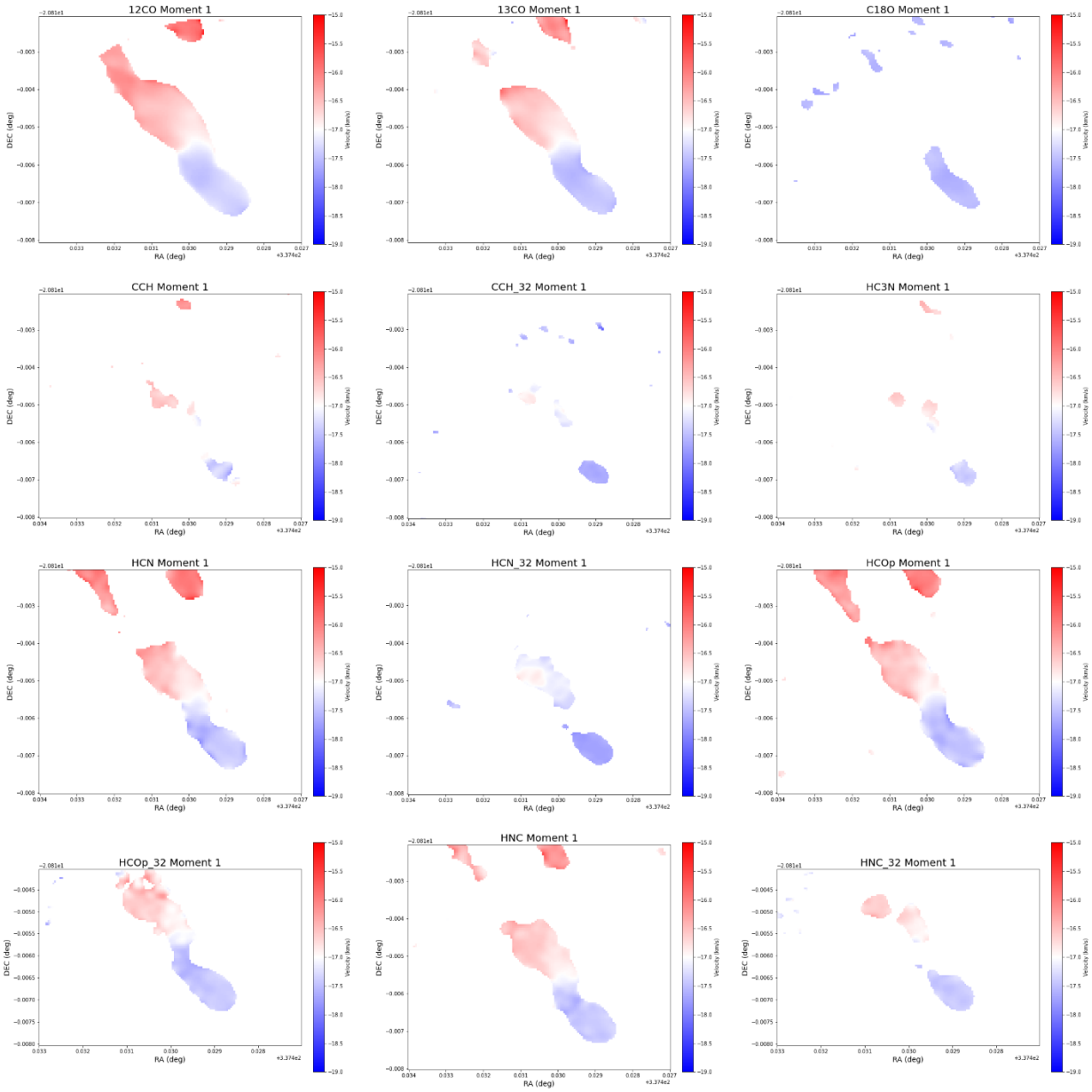

In the Moment 0 maps for Globule B, the red regions indicate where the velocity is redshifted and blue regions indicate blueshift with respect to the central velocity.

Figure 7: Moment 0 Maps for Globule C

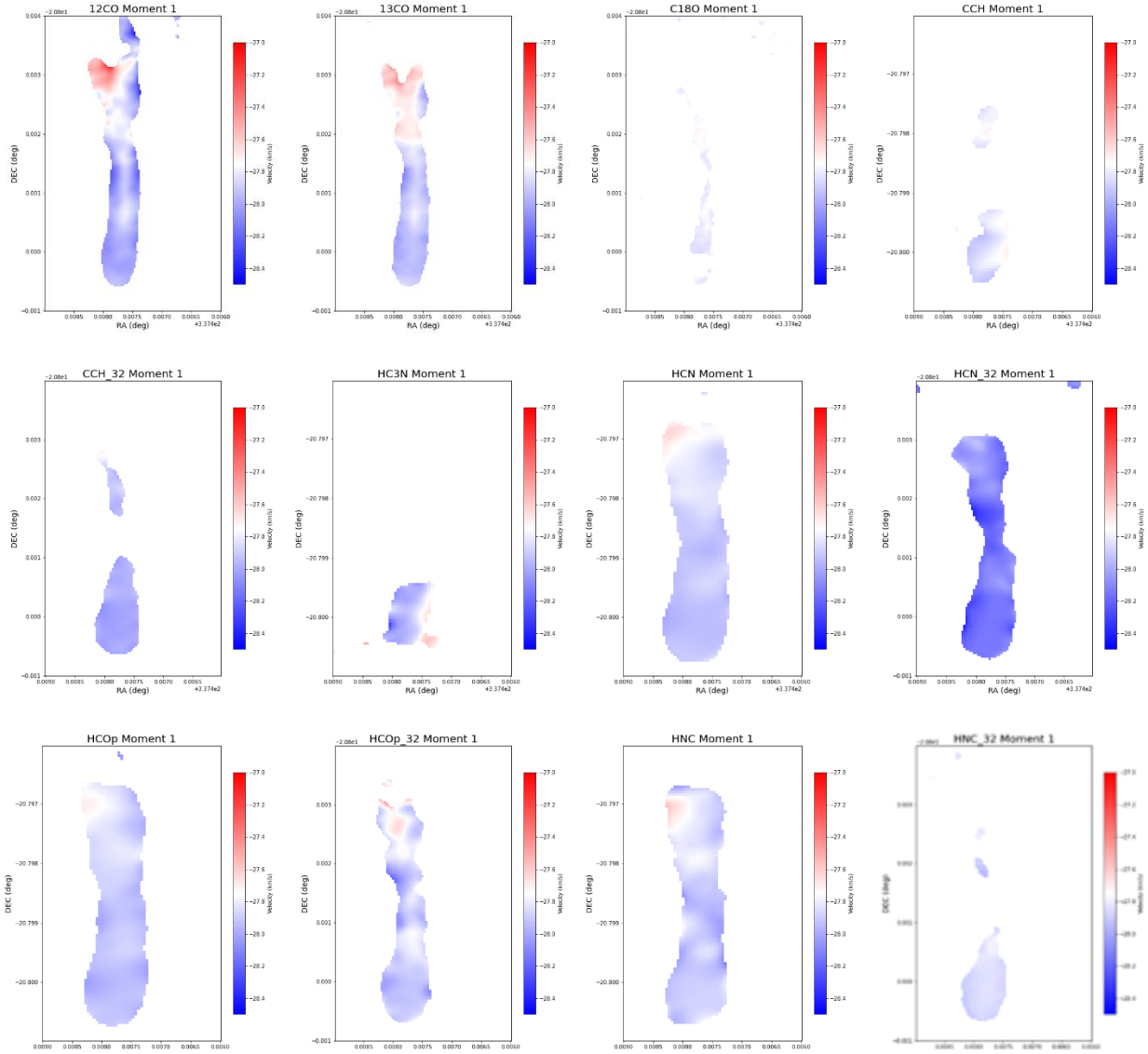

In the Moment 0 maps for Globule C, the red regions indicate where the velocity is redshifted and blue regions indicate blueshift with respect to the central velocity.

C_2H and HCN have multiple hyperfine transitions where the spin of the electron flips causing a split in emitted frequencies (*Table 1*). The velocities were calculated using the rest frequencies, making the multiple hyperfine transitions appear to be moving at different velocities. Not all of the hyperfine lines could be resolved so it is not possible to know if all were detected, as several unresolved lines are clustered together.

3.3: Position Velocity Diagrams

The position velocity diagrams (*Figures 10-11*) depict Globules B and C from a side view by placing the velocity on the x-axis and summing along the right ascension. The globules are not expected to be expanding, so looking at a line of sight, more positive velocities indicate a greater depth from the observer, effectively acting as a physical distance.

Molecule	Hyperfine Transition	Frequency (GHz)
^{12}CO	J = 2→1	230.538
^{13}CO	J = 2→1	220.399
$C^{18}O$	J = 2→1	219.560
C_2H (N = 1→0)	J = 3/2→1/2 F = 1→1	87.28438
	J = 3/2→1/2 F = 2→1	87.31705
	J = 3/2→1/2 F = 1→0	87.32870
	J = 1/2→1/2 F = 1→1	87.40210
	J = 1/2→1/2 F = 0→1	87.40723
	J = 1/2→1/2 F = 1→0	87.44642
C_2H (N = 3→2)	J = 7/2→5/2 F = 4→3	262.00452
	J = 7/2→5/2 F = 3→2	262.00676
	J = 5/2→3/2 F = 3→2	262.06512
	J = 5/2→3/2 F = 2→1	262.06765
HC_3N	J = 11→10	100.076
HCN (J = 1→0)	F = 1→0	88.630413
	F = 2→1	88.631846
	F = 0→1	88.633935
HCN (J = 3→2)	F = 3→3	265.884887
	F = 2→1	265.886185
	F = 3→2	265.886431
	F = 4→3	265.886497
	F = 2→3	265.886976
	F = 2→2	265.888519
HCO^+	J = 1→0	89.188
HCO^+	J = 3→2	267.558
HNC	J = 1→0	90.664
HNC	J = 3→2	271.981

Table 1: Frequencies of Transitions Observed
The above table shows the hyperfine transitions and the frequencies for each transition observed. Values of frequencies of non-hyperfine transitions obtained from the CDMS database. (Tucker (1974), Ziurys (1982), Müller (2005), Mullins (2018))

In the Moment 0 maps and the position-velocity diagrams (*Figures 10-11*), Globule C is broadly vertical. This is demonstrated in the PV diagrams, by being entirely in the same plane, aside from the small ripple at approximately -28.5 km s^{-1}. Additionally, the velocities seen with the position-velocity diagrams for Globule C are close to that of the CSPN, which has a velocity of approximately -25.6775 km s^{-1} (*Meaburn et al., 2008*). This indicates that Globule C is closer to the observer than the CSPN, and is minimally angled from the star (*Table 2*).

The position-velocity diagram for Globule B is consistent with that of the Moment 0 image, suggesting that the globules are radially symmetric about the axis coming from the CSPN. Globule B is angled away from the observer, with the head closer in velocity to that of the CSPN and the tail redshifted. The position-velocity diagram of Globule B also confirms multiple co-spatial components. These can be seen in the three separate groups of contour lines, which represent Globulettes B1, B2 and B3, and B*; B2 and B3 are indistinguishable in this format due to the overlapping declination values. The three globulettes in the main co-spatial component following B1, appear to be somewhat connected by the outer layer of molecules within the 3σ detection in the more extended molecules- ^{12}CO, ^{13}CO, HCN, and HCO^+. However, in the position-velocity diagrams of the less expansive molecules nothing is found to be connecting the globulettes, each appearing at distinct velocities.

All the globules consistently move radially away from the central star in a cometary fashion. A dense molecular head is closest to the CSPN, shielding the rest of the molecules in the tail. Data from the Hubble

Space Telescope [NII] also shows a layer of dense ionized gas in front of the molecular gas further adding to the shielding and cometary nature of the globules. Outside the bounds of the dense molecular gas of the globules, material is highly ionized by the UV radiation from the CSPN. Stellar winds push this gas outwards more readily than the globules, creating their streamlined structure. The globules are also radially symmetric, staying almost entirely behind the dense gas, with respect to the CSPN. The general structure of the globules has led to several possibilities for their formation: that they formed in situ by overdensities in the nebular envelope or that the globules are the remnants of planetary bodies that survived the red giant phase but are now being ablated away. Neither of those possibilities can be confirmed in this study alone.

4: Optical Depth

4.1: Optical Depth Calculations

Assuming local thermodynamic equilibrium (LTE) , the excitation temperature for all the molecules are considered the same (*Andriantsaralaza et al., 2020*). The excitation temperature, T_{ex}, was calculated for ^{12}CO and applied to the optical depth and column density calculations.

$$T_{ex} = 11.06 \left\{ ln\left[1 + \frac{11.06}{T_{peak}+0.19}\right]\right\}^{-1} K \qquad (3)$$

In Globule B, the excitation temperature for ^{12}CO was found to be 23.95 K, with Globule C being 28.93 K. However, an excitation temperature of 24.96 K (calculated by Andriantsaralaza (2020)) was used to avoid uncorrected errors present in the unprocessed archival CO data of Globule C. The main beam temperature was calculated for the molecular detections (*Andriantsaralaza et al., 2020*).

$$T_{mb} = 1.222 \times 10^3 \frac{I}{\nu^2 \theta_{maj} \theta_{min}} K. \qquad (4)$$

The optical depth was calculated for each of the molecular detections. The frequency used to calculate optical depth was the central frequency. To gain the optical depth maps, all parts of the equation relying on a single point, such as the intensity, were replaced with the array of points within a 3σ detection to plot over the same region.

$$\tau = -ln\left\{1 - \frac{T_{mb}k}{h\nu}\left[\frac{1}{exp\left(\frac{h\nu}{kT_{ex}}\right)-1} - \frac{1}{\left(exp\left(\frac{h\nu}{2.73k}\right)-1\right)}\right]^{-1}\right\} \qquad (5)$$

4.2: Optical Depth Maps

The Optical Depth maps (*Figures 12-13*) indicate variation in the opacity of the molecules. Any point with an optical depth at or above one would be considered optically thick, while an optical depth well below one being considered optically thin. In the cases where the globule is optically thick, only the surface of the globule is seen because only photons near the surface can escape without scattering and thus losing information about their origin . Where it is optically thin, it is possible to see all the way through the globule, which is beneficial when examining the column density.

Most of the molecules' optical depths are well below 1, consistently with $\tau < 0.45$ (*Figures 12-13*), indicating that they are optically thin. The only molecule that is consistently optically thick is ^{12}CO, having optical depth values upwards of 5.35 in Globule C and 1.46 in Globule B. HCN is also optically thick in some regions ($\tau = 0.66$ Globule C and $\tau = 1.05$ Globule B). There is a notable difference between the maximum optical depths of these two globules, which appears to be primarily due to the difference in

data reduction processes. When calculating the optical depth of ^{12}CO in Globule C, there were also some issues that lead to the number of velocity channels being included in the integrated intensity being changed. The uncharacteristically bright spots in the tail of Globule C seen in ^{12}CO caused errors during calculations, resulting in negatives inside of the natural logarithm. To mitigate this, the number of velocity channels included was reduced to include only the most significant points. The bright point in the tail of Globule C where the optical depth is highest in ^{12}CO was the source of Point 3 (*Figure 4*).

5: Column Density

As most of the molecules showed an optically thin medium, the assumption during column density calculations was made that all the media were optically thick (*Andriantsaralaza et al., 2020*). The first part of the column density calculation (equation 6) is an approximation for the partition function (*Nishimura et al., 2015*).

$$Z = \frac{kT_{ex}}{hB_0} + \frac{1}{3} \quad (6)$$

The complete equation for column density used in this study is seen below in equation 7 and has units of cm^{-2} (*Andriantsaralaza et al., 2020*).

$$N = \frac{\frac{8\nu_0^3 Z}{A_{lu}c^3}\left[exp\left(\frac{h\nu k}{T_{ex}}\right)-1\right]\left[exp\left(\frac{hB_0 J(J+1)}{kT_{ex}}\right)\right]\int \tau(v)dv}{2J+1} \quad (7)$$

This equation gives an approximation for the number of molecules per square centimeter for each pixel. For the column density maps (*Figures 14-15*) the integrated intensity was used and the equation was applied to all the points across the 3σ detection, rather than to a single point.

The column density maps (*Figures 14-15*) are qualitatively the same as the optical depth maps as they are only a scale factor of the same maps. For the ^{12}CO column density map, the assumption was made that the column density was 10 times that of ^{13}CO to avoid the change made in section 4.2 where some of the relevant channels were excluded in the Globule C calculation and to account for the assumption that ^{12}CO was optically thick and the assumption was made that the media were optically thin (*Andriantsaralaza et al., 2020*).

6: Line Ratios

To calculate the line ratio maps for each of the comparisons desired, the pixels were redefined to match each other as the beam size varied with of the molecular detections, changing the number of pixels and pixel sizes for each molecule. The pixel size and extent of the image was defined by the molecule or transition in the denominator of the ratio to avoid errors dividing by zero. Due to the shape of two data cubes, the J = 3→2 transition of HNC and HCO^+ images of Globule B are missing part of the globule tail present in other images. For this reason, the line ratio maps were limited in scope. After the rescaling of the image pixels of the Moment 0 maps, the selected pairs of molecules were divided, and the quotients plotted . The line ratio maps (*Figure 16*), show comparisons of the isotopologues of CO as well as the two transitions of C_2H, HCN, HCO^+, and HNC.

Comparing different transitions of the same molecule, the higher transition (J=3-2) is more prevalent at the head of the globule, closest to the CSPN. Further back, this higher frequency transition decreases in intensity, though still more prevalent than the lower frequency J=1—0 transition. This suggests that the energy needed to induce higher molecular

transitions is absorbed predominantly at the font surface of a globule, allowing the ratio to be lower deeper within the gas cloud. Additionally, some of the edges further in the back that peek out from protective layers of proceeding gas are also seen to have a stronger intensity of higher frequency emitting molecules and therefore have brighter areas in the line ratio maps. This is because those areas do not have anything in front of them to absorb the radiation as is seen in the front of the head. In most parts of the edges of the globules stay within the bounds of the front of the head as outside of these edges most of the molecules are directly exposed to the harsh direct UV radiation, which breaks most molecular bonds in those areas. Where there is a small amount of wiggle on the edges is heavily dominated by molecules emitting higher frequencies because they are being directly exposed to the shorter wavelengths of the UV radiation from the CSPN.

There is also a noteworthy line ratio map comparing the isomers HCN and HNC (*Figure 17*). Despite the similar molecular structure of HCN and HNC, the column density maps reveal an average column density of 9.85×10^{12} and 3.84×10^{12} respectively for Globule B and 3.77×10^{12} and 1.85×10^{12} for Globule C, with these values being for the J=1→0 transition only, though the trend is the same for J=3→2 *(Figures 14-15*). This is because of the difference in energies required to separate the hydrogen atom from the cyanide ion. HNC requires slightly less energy to break off the hydrogen atom, at which point the hydrogen can rebond to either side of the cyanide. Assuming a relatively equal chance of the lone hydrogen bonding to either side of the cyanide, and given the additional energy needed to break apart HCN, HNC will preferentially be converted to HCN, thus leading to a higher abundance of the molecule. This comparison is also seen in the line ratio maps comparing the intensity of the emission between the J=1→0 transitions of HCN and HNC in both globules B and C (*Figure 17*). In agreement with the discussion of the column densities, the ratio of HCN:HNC is nearly constant throughout the entire globule, with HCN consistently having 2-3 times higher intensity emission than HNC. This very constant ratio indicates how the uneven potential well has a consistent impact on their entirety of the globules.

Figure 17: Line Ratio Maps for HCN/HNC (1-0)

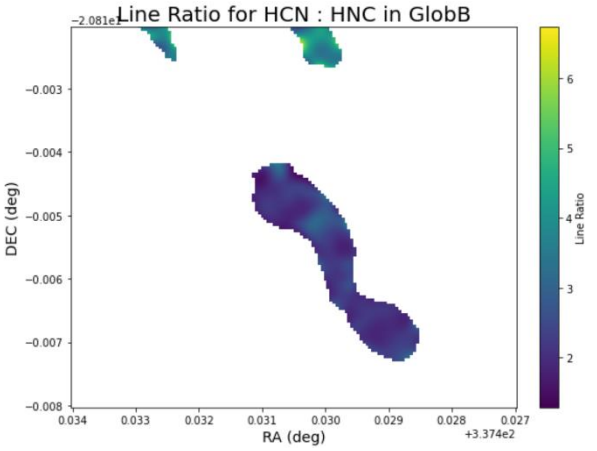

The line ratio map comparing the intensity of the emission from the J=1→0 transition of HCN/HNC for Globule B show that the ratio is nearly constant throughout both globules, with HCN being more prevalent.

7: Distance and Mass Calculations

7.1: Distance Calculations

The distance was calculated for six points in Globule B and for three points in Globule C (*Figure 4*). To begin, the distance on the plane from the central star to each of the points using the J2000 right ascension and declination coordinates for the CSPN. These coordinates were (337.4125, -20.8372), (*Gaia Collaboration, 2021*).

The distance into the plane of the sky was then calculated based primarily on the change in velocity from the CSPN to the velocity of each noted point in the globules (*Figure 4*). The distance to the CSPN was taken to be 199.6 pc (*Gaia Collaboration, 2021*). The velocity of the CSPN was taken to be -25.6775 km s^{-1} (*Meaburn et al., 2008*). The expansion rate for the ionized region of the Helix Nebula is taken to be 14 km s^{-1} *(Meaburn et al., 2005)*. The angle to the CSPN was also calculated (*Table 2*).

The angles shown for the points in Globule B are consistent with the idea that Globule B is substantially angled away from the CSPN with Globulettes B2, B3, and B* being at a slightly greater angle to the CSPN than B1, which was also observed in the Position-Velocity Diagrams. Globule C is much more vertical, but the angles observed have more variation, likely due to the wiggle along the velocity axis, noted in the position velocity diagrams.

Point	Distance from CSPN (parsecs)	Angle to CSPN (degrees)
B1	0.1116	35.460
B2	0.1159	35.463
B3	0.1263	39.182
B4	0.1311	40.087
B5	0.1443	41.124
B6	0.1472	43.770
C1	0.1322	9.726
C2	0.1402	7.502
C3	0.1432	10.722

Table 2: Distances and Angles for Points
The distances and angles with respect to the central star of the planetary nebula of the points labeled in Figure 3.

7.2: Mass Calculations

The masses of each of the globules were calculated based on the column density of ^{13}CO and the pixel size. ^{13}CO was chosen because it was optically thin and had known estimates for a ratio of ^{13}CO to ^{12}CO (*Andriantsaralaza et al., 2020*). The assumption of a CO: H_2 ratio of 6×10^{-4} was used to estimate the mass of the entire globule (*Huggins et al., 1992, 2002*). The pixel size in arcseconds was converted to cm^2 and multiplied by the average column density of the entire globule and the number of pixels present within a 3σ detection. This product would give the number of ^{13}CO molecules in the globule. This number can then be used in a 1:10 ratio to calculate the number of ^{12}CO molecules inside of each of the globules (*Andriantsaralaza et al., 2020*). Once the number of H_2 molecules was calculated, the molecular mass of the molecular hydrogen was found and then converted to solar masses, thereby giving the values of 7.56×10^{-5} $M_\odot$ for Globule B and 3.13×10^{-5} $M_\odot$ for Globule C.

8: Conclusions

This study suggests that the structure of the globules is approximately the same for each molecule across both of the globules examined in the Helix Nebula. Both globules contain a dense head closer to the CSPN followed by a diffuse tail that extends in a cometary fashion almost exclusively behind that dense molecular head. Within the structure of both Globules B and C, larger molecules such as HC_3N and HCO^+ are found almost exclusively in the densest regions, as these are the best conditions for the formation and survival of these molecules.

The line ratios between two transitions of the same molecule indicate higher energy transitions are more prevalent nearer to the CSPN, scattering higher frequency radiation and allowing lower energy transitions to be more prevalent in the back of the head of the globule and in the tail. Comparing the isomers

of HCN and HNC also reveals a near constant ratio between the two, having qualitatively near identical structures, and HCN consistently being more prevalent as it requires more energy to break the bond between the hydrogen ion and the cyanide ion than HNC.

Future works in this area are to approximate the age of the globules by examining the chemical reactions required for the detected chemical composition and the length of time it would take to reach this state from the AGB phase of stellar evolution. In looking at the age and chemical reactions, the origin of the globules would also be examined as would the future evolution of the chemical composition of the globules in the Helix Nebula.

9: Acknowledgements

This paper makes use of the following ALMA data: ADS/JAO.ALMA# 2018.1.01006.S and 2012.1.00116.S. ALMA is a partnership of ESO (representing its member states), NSF (USA) and NINS (Japan), together with NRC (Canada), MOST and ASIAA (Taiwan), and KASI (Republic of Korea), in cooperation with the Republic of Chile. The Joint ALMA Observatory is operated by ESO, AUI/NRAO and NAOJ. The National Radio Astronomy Observatory is a facility of the National Science Foundation operated under cooperative agreement by Associated Universities, Inc.

In addition, the authors would like to thank the GBO and W. Armentrout for their support of this project during the 2021 Summer REU.

10: References

Andriantsaralaza M., Zijlstra A., Avison A., 2020, MNRAS, 491, 758

Bachiller R., Forveille T., Huggins P., Cox P., 1997, Astronomy and Astrophysics, 324, 1123

Gaia Collaboration et al., 2021

Huggins P., Mauron N., 2002, Astronomy & Astrophysics, 393, 273

Huggins, P. J., Forveille, T., Bachiller, R., Cox, P., Ageorges, N., & Walsh, J. R. 2002, ApJ, 573, L55

Huggins P., Bachiller R., Cox P., Forveille T., 1992, The Astrophysical Journal, 401, L43

Nishimura A., et al., 2015, The Astrophysical Journal Supplement Series, 216, 18

Ziurys, L. M., Saykally, R. J., Plambeck, R. L., & Erickson, N. R. 1982, ApJ, 254, 94

11: Appendices

Figure 8: Spectral Lines for Globule B

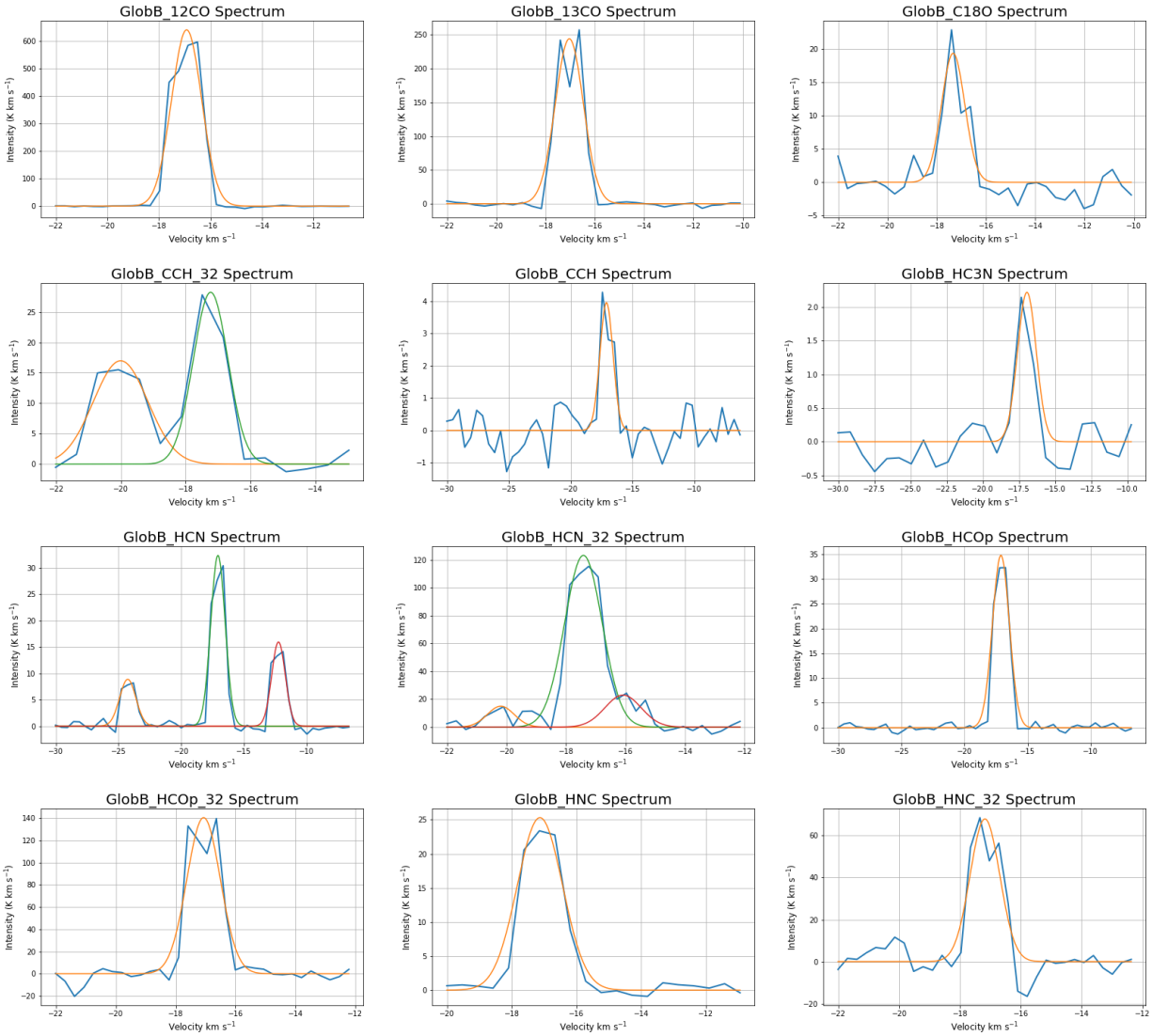

The spectra (blue) each show their accompanying gaussian fits (orange, green, red) for all 12 of the molecules detected in Globule B.

Figure 9: Spectral Lines for Globule C

The spectra (blue) each show their accompanying gaussian fits (orange, green, red) for all 12 of the molecules detected in Globule C.

Figure 10: Position-Velocity Diagrams for Globule B

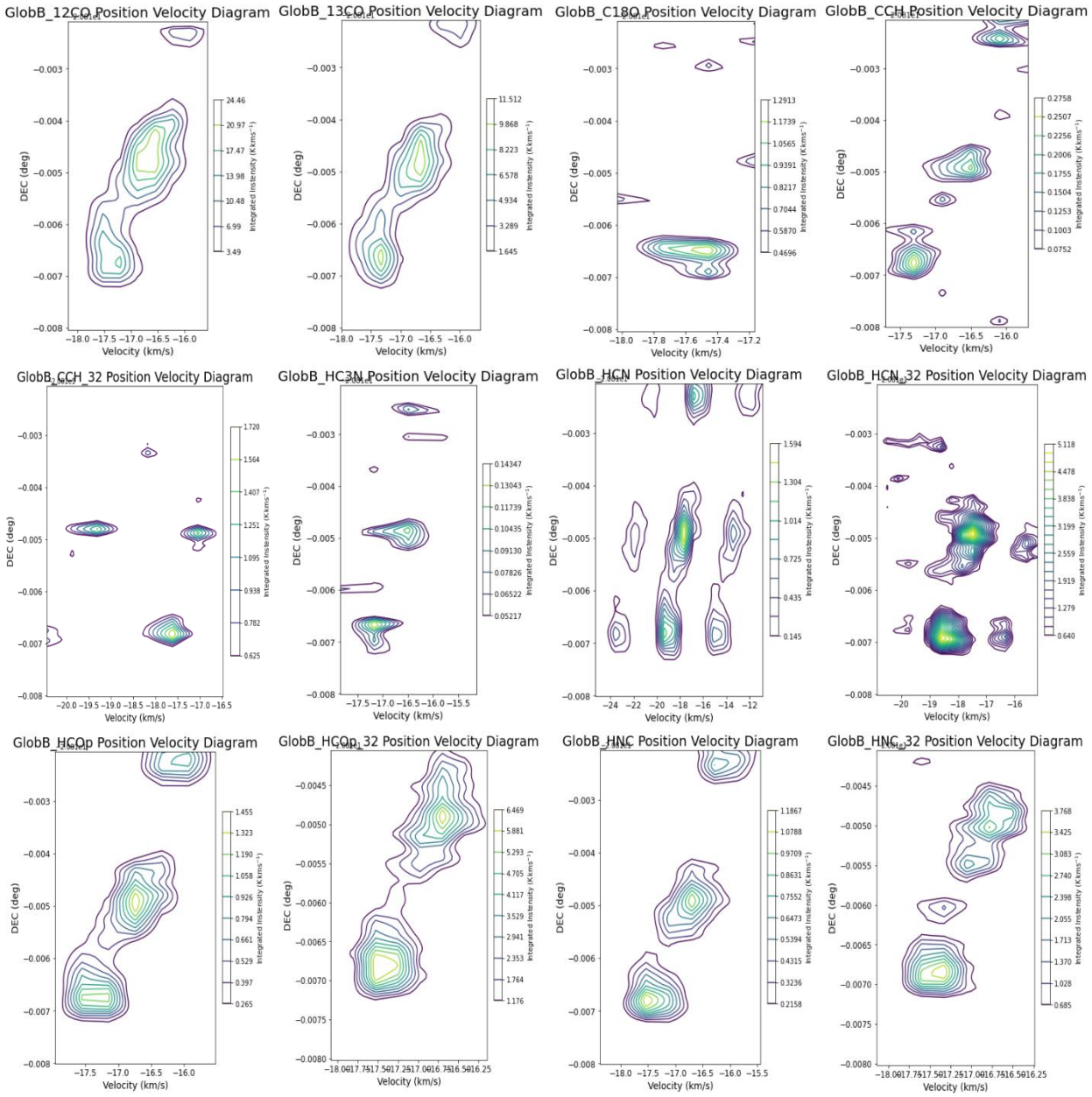

The position-velocity diagrams for Globule B use velocity as a space variable, plotting the intensity, integrated along the right ascension, against the velocity and the declination to effectively show an estimate of the globules seen from the side. The multiple hyperfine transitions are depicted as multiple globules side by side.

Figure 11: Position-Velocity Diagrams for Globule C

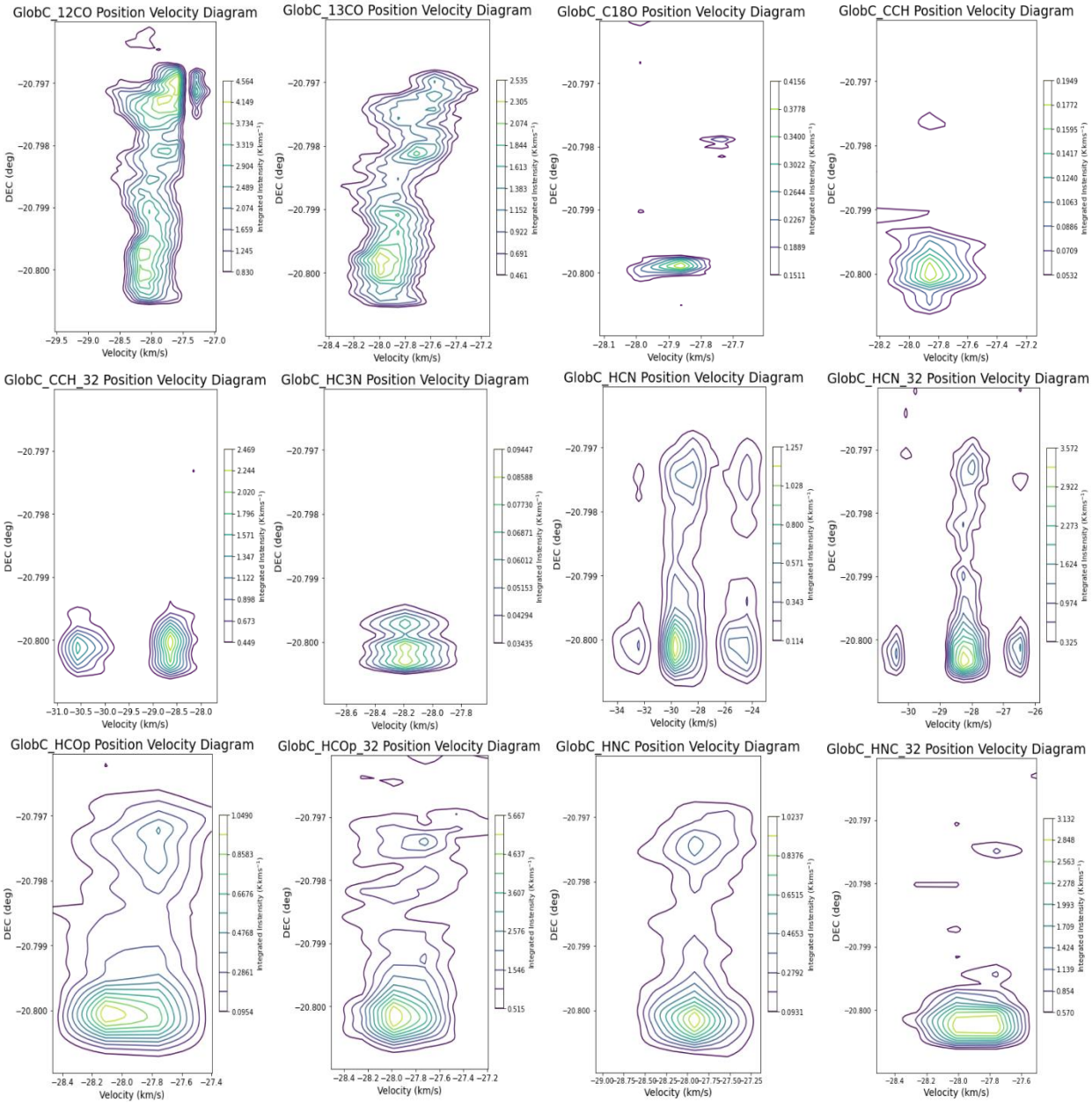

The position-velocity diagrams for Globule C use velocity as a space variable, plotting the intensity, integrated along the right ascension, against the velocity and the declination to effectively show an estimate of the globules seen from the side. The multiple hyperfine transitions are depicted as multiple globules side by side.

Figure 12: Optical Depth Maps for Globule B

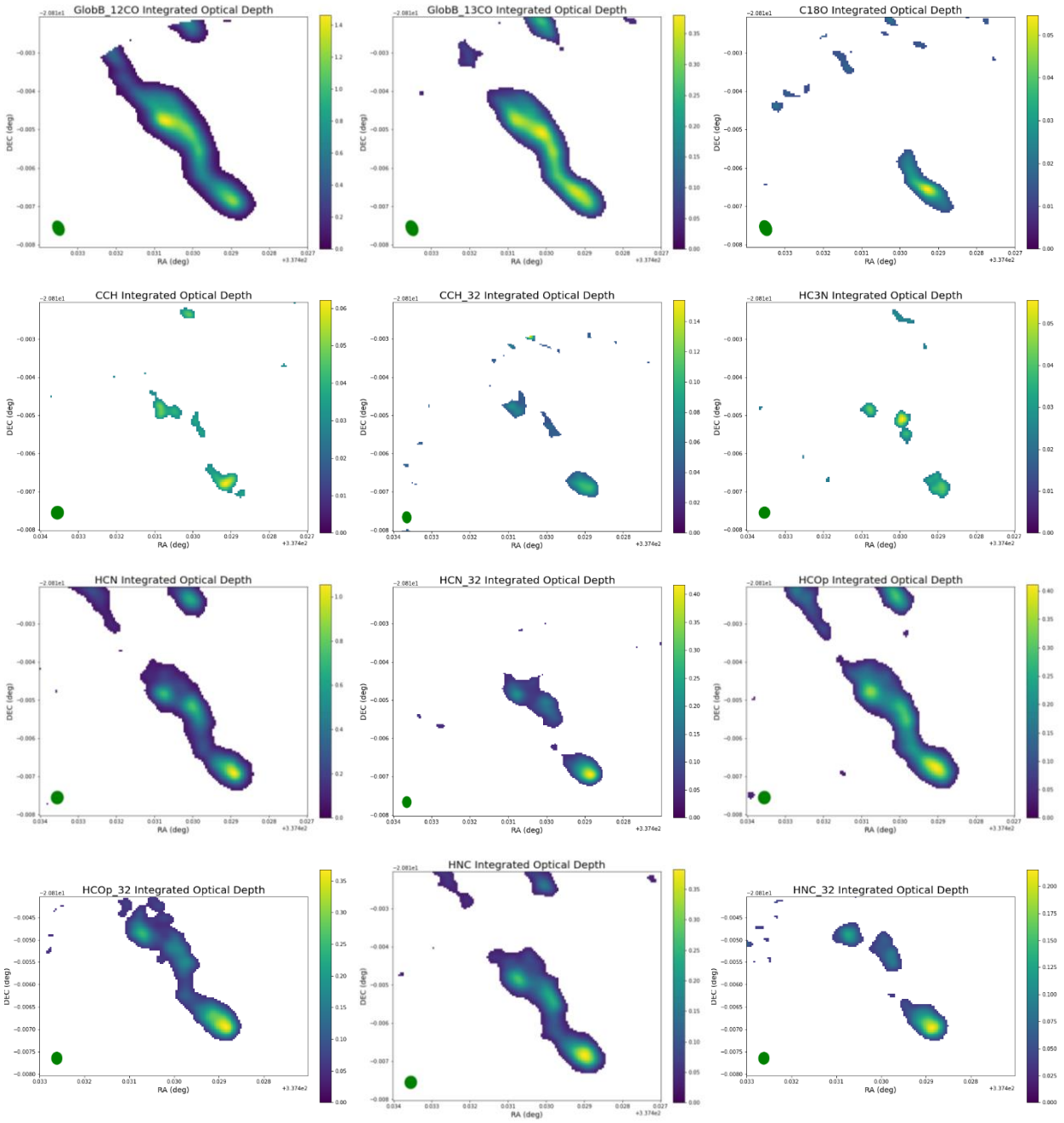

The optical depth maps illustrate the change in opacity of Globule B, with only ^{12}CO and parts of HCN being optically thick. All of the other molecular detections are optically thin.

Figure 13: Optical Depth Maps for Globule C

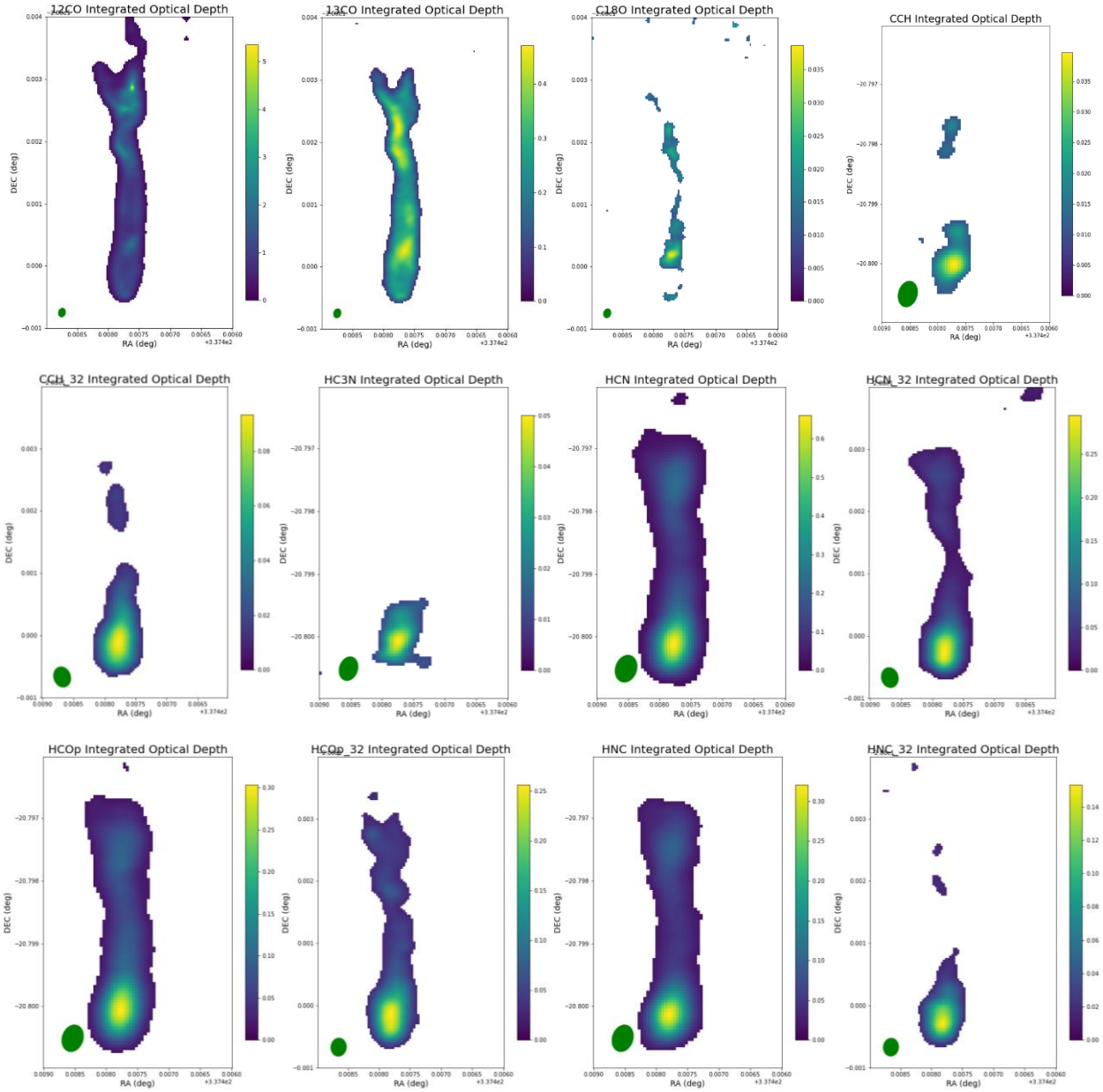

The optical depth maps illustrate the change in opacity of Globule C, with only ^{12}CO and parts of HCN being optically thick. All of the other molecular detections are optically thin.

Figure 14: Column Density Maps for Globule B

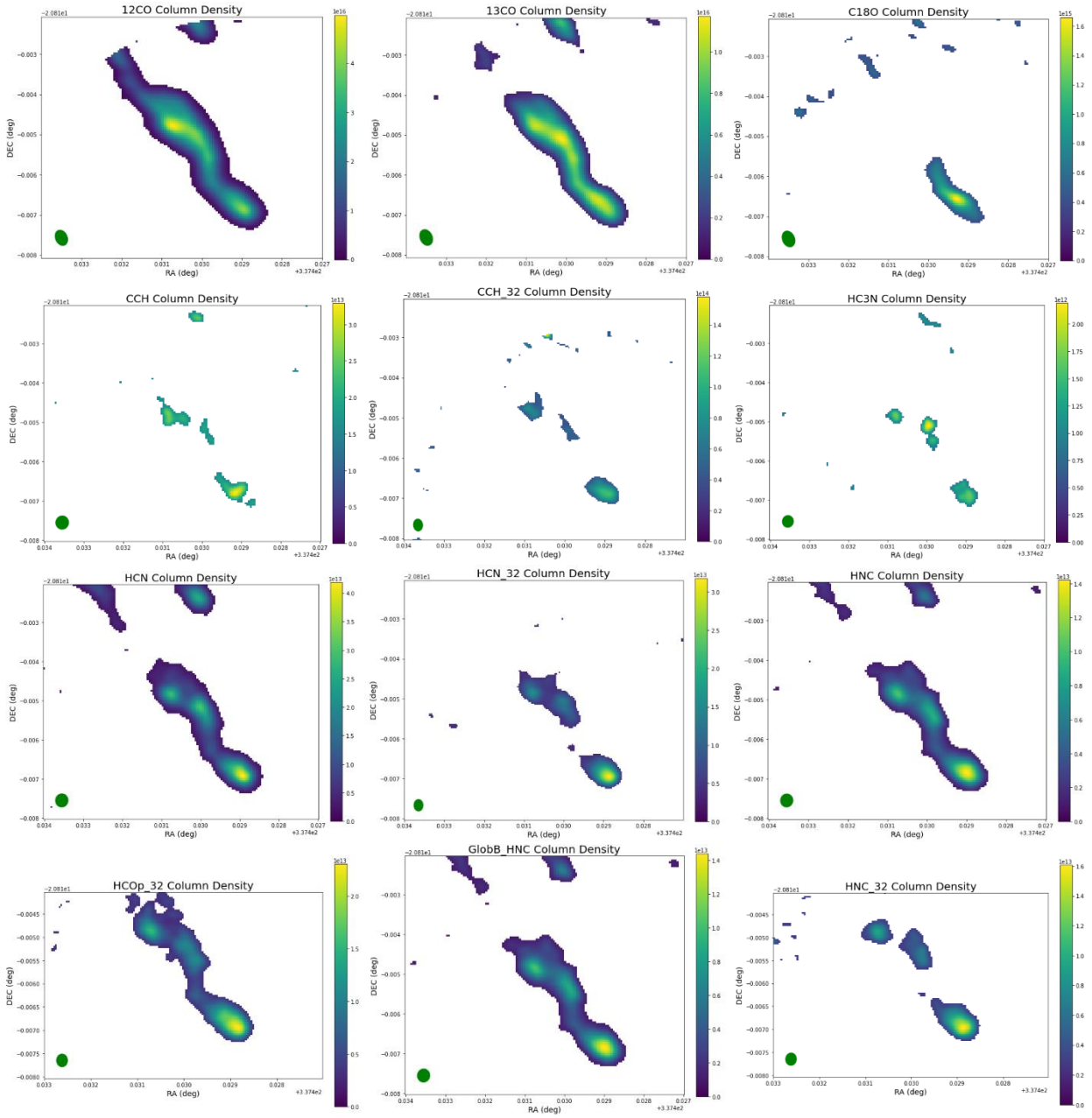

The column density maps for Globule B show an approximation as to how many molecules per cm^2 are along each line of sight, using an assumption that the globule is optically thin for each calculation.

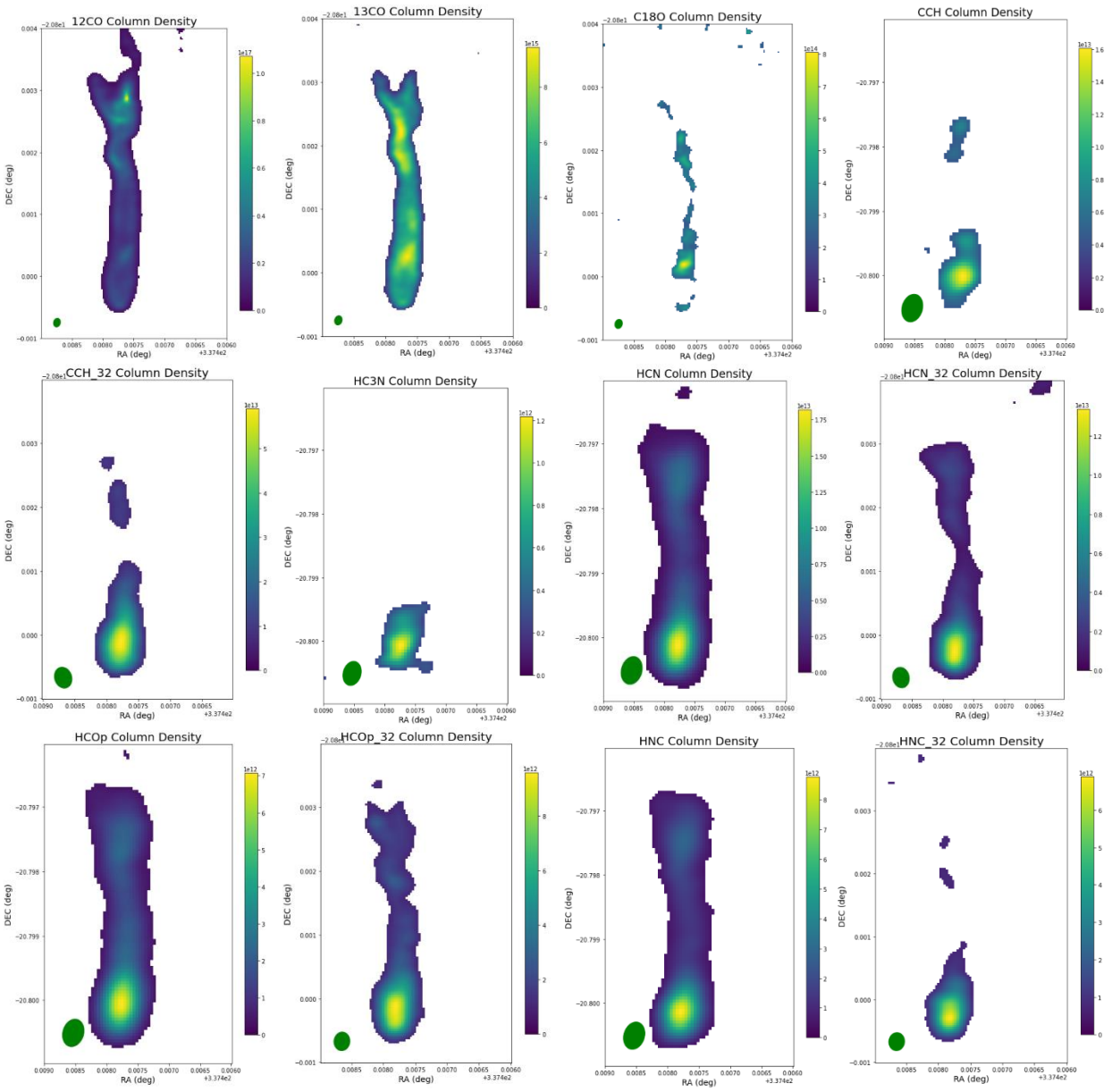

The column density maps for Globule C show an approximation as to how many molecules per cm^{-2} are along each line of sight, using an assumption that the globule is optically thin for each calculation.

Figure 16: Line Ratio Maps Comparing Transitions of the Same Molecule

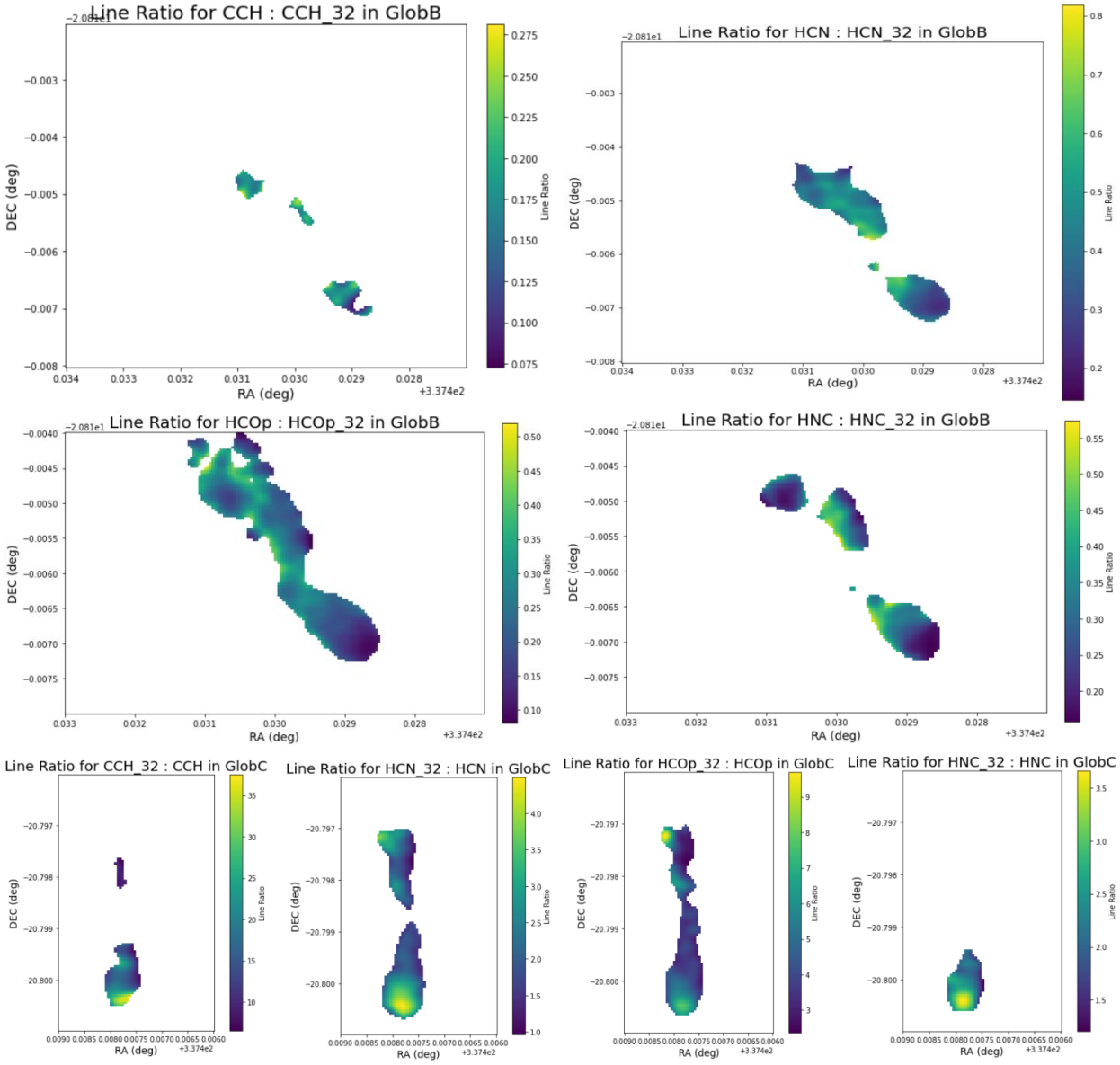

The above images show the line ratio maps for the intensity of the 3-2 transition to the intensity of the 1-0 transition for all of the molecules where these two transitions were detected- those being C_2H, HCN, HCO^+, and HNC. These maps are shown for Globule B above and Globule C below.